INTERACTIONS BETWEEN CELLULOSE ETHERS AND A BILE SALT IN THE CONTROL OF LIPID DIGESTION OF LIPID-BASED SYSTEMS

Amelia Torcello-Gómez[a,*] and Timothy J. Foster[a]

[a]Division of Food Sciences, School of Biosciences, University of Nottingham, Sutton Bonington Campus, Loughborough, LE12 5RD, United Kingdom, email addresses: amelia.torcello_gomez@nottingham.ac.uk, tim.foster@nottingham.ac.uk

Corresponding author (*): Division of Food Sciences, School of Biosciences, University of Nottingham, Sutton Bonington Campus, Loughborough, LE12 5RD, United Kingdom

Email address: amelia.torcello_gomez@nottingham.ac.uk (A. Torcello-Gómez)

Tel: +44 (0)115 951 6197

Fax: +44 (0)115 951 6142

ABSTRACT

In order to gain new insights into the potential of specific dietary fibres to control lipid digestion, the goal of this work is to study the main interactions between commercial cellulose ethers, as dietary fibre, and a bile salt, as an important duodenal component present during the digestibility of lipids. These interactions have been evaluated in two different scenarios found for an oil-in-water emulsion on its transit through the duodenum. Namely, interactions in the continuous phase and competitive adsorption at the oil–water interface have been looked at by means of micro-differential scanning calorimetry (micro-DSC) and interfacial tension (IT). Micro-DSC revealed that the presence of the bile salt affects the thermogelation process of cellulose derivatives, suggesting binding to cellulose ethers. The effect on thermogelation seems to be cellulose type-dependent. IT measurements proved the ability of cellulose ethers to compete for the oil–water interface in the presence of the bile salt. Interactions in the bulk might have an impact on this interfacial scenario. These findings may have implications in the digestion of emulsified lipids, hence providing a springboard to develop new cellulose-based food products with improved functional properties.

Keywords: dietary fibre, cellulose ethers, bile salts, oil–water interface, interfacial tension, differential scanning calorimetry.

52 1. INTRODUCTION

53 Cellulose derivatives belong to a wide group called dietary fibres which have been shown to
54 provide health benefits in the diet by, for instance, lowering blood cholesterol (Anderson &
55 Siesel, 1990; Kritchevsky & Story, 1993). This is due to the ability of certain types of dietary
56 fibre to interfere with the process of digestion in a number of different and related ways. On
57 the one hand, dietary fibres bind bile salts in the duodenum which are sequestered and
58 eventually excreted (Story, Furumoto, & Buhman, 1997). Hence, dietary fibres reduce bile
59 re-absorption, inducing the synthesis of bile salts from blood cholesterol to restore the content
60 lost (Lee, Kim, & Kim, 1999; Zarras & Vogl, 1999). On the other hand, an alternative
61 mechanism proposed to explain the reduction of blood cholesterol levels by dietary fibre is
62 the prevention of lipid absorption (Jenkins, Kendall, & Ransom, 1998; Lairon, 1996;
63 Yokoyama et al., 2011), which can be partially related to the sequestration of bile salt due to
64 binding. Indeed, the binding mechanism may influence lipid absorption by affecting the
65 process of lipid digestion. This is because bile salts play a crucial role in lipid digestion
66 within the duodenum (upper small intestine), where the majority of this process occurs, *c.a.*
67 70-90% (Fave, Coste, & Armand, 2004). When lipids eventually reach the small intestine,
68 they are normally present as small lipid droplets dispersed in a compositionally and
69 structurally complex aqueous medium. Bile salts are secreted into the duodenum and adsorb
70 onto the surface of lipid droplets to further emulsify them and to prepare this interface for the
71 enzymatic breakdown by the pancreatic lipase. This enzyme anchors to the lipid-water
72 interface with the help of its cofactor colipase, previously adsorbed on the bile salt-covered
73 interface, by forming a lipase-colipase complex (Reis, Holmberg, Watzke, Leser, & Miller,
74 2009). Lipase then hydrolyses the lipids (lipolysis), mainly composed of triglycerides, into
75 free fatty acids, monoglycerides and diglycerides. Some of these products are soluble, so that

76 they can be removed from the surface of lipid droplets and become incorporated within
77 micelles/vesicles of bile salts in order to be absorbed by the intestinal mucosa.
78 Therefore, any way whereby dietary fibre can interfere with the above process may also
79 affect the rate of lipid digestion and hence absorption. Several possible mechanisms that may
80 alter this process include the binding of dietary fibre to bile salts or to the enzymes, the
81 adsorption of dietary fibre on the oil–water interface, forming a protective layer against the
82 action of bile salts and lipase, and intraluminal disruption of mixed micelles of digested lipids
83 and bile salts, reducing transport into the mucosal surface barrier (Vahouny et al., 1988).
84 Despite the known ability of dietary fibres to influence lipid absorption, to our best
85 knowledge there is a need of fundamental studies on their potential to control lipid digestion
86 (Beysseriat, Decker, & McClements, 2006; Tokle, Lesmes, Decker, & McClements, 2012).
87 Previous work in literature reported on electrostatic interactions between chitosan and a bile
88 salt (Thongngam & McClements, 2005), dynamic molecular contact of beta-glucan with a
89 bile salt and entrapment of bile micelles by an arabinoxylan matrix without direct molecular
90 interaction (Gunness, Flanagan, & Gidley, 2010). However, the mechanisms by which dietary
91 fibres interact with bile salts in the digestive tract are still not known. Hence, a systematic
92 approach should be taken to identify the dominant mechanism for each specific type of
93 dietary fibre to influence lipid digestion, in order to better understand the underlying
94 molecular effects of digestion conditions in real complex food emulsions containing specific
95 dietary fibres.
96 A previous study on the interactions between synthetic polymeric surfactants and bile salts in
97 oil-in-water emulsions has shown that binding of these polymers to a bile salt may have an
98 impact on the interfacial properties of the emulsions related to access for digestion (Torcello-
99 Gómez, Maldonado-Valderrama, Jódar-Reyes, & Foster, 2013). Cellulose derivatives offer a
100 good candidate mirroring the block-copolymer research. For that reason, the aim of this work

is to study the main interactions between cellulose derivatives, as non-ionic dietary fibre, and bile salts, as an important duodenal component. Specifically, we have focused on the interactions in the aqueous phase and competitive adsorption at the oil–water interface as scenarios of oil-in-water emulsions as they pass through the duodenum. These interactions have been characterised in the aqueous phase by means of micro-differential scanning calorimetry, and at the oil–water interface through competitive adsorption by means of interfacial tension measurements. This combination of techniques has shown to be successful in previous work (Torcello-Gómez et al., 2013).

Commercial cellulose ethers have been chosen as dietary fibre due to the highly functional properties which are important in the manufacture process of food, such as: surface activity, binding, thickening, and a wide range of viscosities. For the cellulose derivatives chosen, the native cellulose backbone has been chemically modified by partially reacting the hydroxyl groups in each sugar ring (Table 1) to provide the following cellulose ethers: methylcellulose (MC), in which methyl group is the sole substituent, hydroxypropylmethylcellulose (HPMC) in which methyl group remains the dominant substituent, but incorporating smaller amounts of the larger and more polar hydroxypropyl group, and hydroxypropylcellulose (HPC) where the hydroxypropyl group is the sole substituent. These are three of the four cellulose derivative forms used in the food area for their surface tension reducing properties (Mezdour, Cuvelier, Cash, & Michon, 2007). This selection allows us to discuss the results comparing their molecular properties, such as the molecular weight in the case of MC, and the type and number of substituents for a set of cellulose ethers within the same range of viscosity (MC, HPMC and HPC) and hence molecular weight (see Table 1), since the viscosity of aqueous solutions of cellulose ethers is proportional to its molecular weight. Sodium taurodeoxycholate (NaTDC) was used as an example of a typical bile salt, since bile salts

behave in a qualitative similar manner despite their large variety (Maldonado-Valderrama, Wilde, Macierzanka, & Mackie, 2011).

Beginning to quantify the dynamics of interactions in the bulk and the impact that has on the interfacial properties, related to access for digestion, provides new insights for designing rules for application. These new findings can be exploited in tailoring both novel food and pharmacological matrices with improved functional properties.

Table 1. Physicochemical characteristics of the cellulose ethers (Sarkar, 1979).

Cellulose Ether		$DS_{methoxyl}$	$MS_{hydroxypropyl}$	Viscosity range (mPa·s)	MW range (KDa)
MC	A4C	1.8	0	400 (2 wt%)	120-150
	A4M			4000 (2 wt%)	300-500
HPMC	K4M	1.4	0.21	4000 (2 wt%)	300-500
HPC	HF	0	4	1500-3000 (1 wt%)	1115

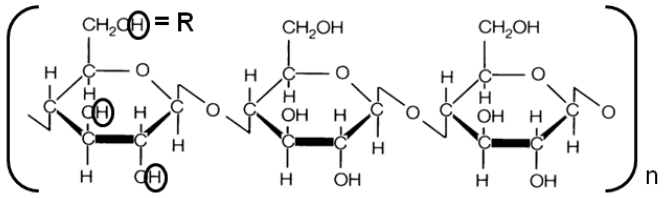

MC: R = H or -CH_3
HPMC: R = H, -CH_3 or -$CH_2CH(OH)CH_3$
HPC: R = H or -$CH_2CH(OH)CH_3$

2. MATERIALS AND METHODS

2.1. Materials

METHOCEL™ A4C, A4M and K4M from the Dow Chemical Company were used without purification. The initial letter 'A' denotes MC and 'K' corresponds to HPMC. In each case, '4C' and '4M' denote a solution viscosity of 400 and 4000 mPa·s, respectively, measured at

2 wt% concentration under standard conditions in a capillary viscometer. Klucel® HPC HF was purchased from Hercules. The different levels of incorporation of the two substituents (degree of substitution, DS, and molar substitution, MS) and range of viscosities are indicated in Table 1.

The bile salt used in this study is sodium taurodeoxycholate (NaTDC, 97% purity) from Sigma-Aldrich. It is negatively charged at pH 7 and its molecular weight is 521.7 g/mol.

The aqueous phase was 1.13 mM phosphate buffer (pH 7) prepared with ultrapure water purified in a Pur1te Select system.

Highly refined olive oil was also purchased from Sigma-Aldrich, and purified with activated magnesium silicate (Florisil®, Fluka) to eliminate free fatty acids and surface active impurities. Namely, a mixture of oil and Florisil® in proportion 2:1 wt/wt was shaken mildly for 3 h and centrifuged at 4000 rpm for 30 min in a bench centrifuge. It was then filtered through Whatman filter paper #1 under vacuum and stored away from light.

2.2. Sample Preparation

Cellulose ethers stock solutions (2 wt%) were prepared as follows. Approximately one-third of the required final volume of aqueous phase was heated to ~80 °C, and then cellulose ether powder was added carefully under stirring. The complete solubilisation was obtained by adding the remaining aqueous phase at room temperature and continuing the agitation of the solution for at least 2 h at room temperature. It was then stored at 4 °C overnight to achieve the maximum hydration, and without stirring to eliminate air bubbles. Aliquots from the stock solutions were dried at 50 °C overnight to confirm that the final concentration was 2 wt%. Different concentrations were obtained by successive dilution from the concentrated stock.

NaTDC stock solution was prepared by dissolving the powder in the aqueous phase at room temperature under stirring for at least 1 h. Then, the stock solution was successively diluted to obtain different concentrations.

Mixed cellulose ethers-NaTDC solutions were prepared from aliquots of cellulose ethers and NaTDC solutions at room temperature, in various proportions. The final concentration of cellulose ethers was fixed at 0.3 and 1 wt% for micro-DSC experiments and at 10^{-3} wt% for interfacial tension measurements, whereas the final concentration of NaTDC ranged from 0 to 100 mM.

2.3. Micro-Differential Scanning Calorimetry (micro-DSC)

The bulk properties of cellulose ethers in the absence and presence of bile salt were studied by characterising the thermal events of the samples in a Micro-Differential Scanning Calorimeter (DSC III Setaram, Caluire, France). About 800 mg of each sample were sealed into the DSC cells made from Hastalloy. The reference cell was filled with the same weight of phosphate buffer and coordinated for heat capacity with the sample. Sample and reference cells were initially cooled to a starting temperature of 5 °C to equilibrate. Cells were then run at a scanning rate of 1 °C/min from 5 to 110 °C, cooled and rerun while all steps were recorded. The heating rate was selected as a compromise between the need for proximity to the equilibrium (heating rate as low as possible) and an acceptable signal/disturbance ratio (heating rate not too low). Enthalpy values were calculated using Setaram software with a linear interpolated baseline, based on an extension of the trace before and after the thermal event.

2.4. Interfacial Tension and Dilatational Rheology

188 Adsorption of cellulose ethers at the olive oil–water interface, alone or in competitive
189 adsorption with the bile salt, was characterised by means of a Profile Analysis Tensiometer
190 (PAT1, SINTERFACE Technologies, Germany). For this purpose, the interfacial tension was
191 recorded at constant interfacial area during 30 min. The apparatus is computer-controlled; the
192 software fits the experimental drop profile to the Young-Laplace equation of capillarity
193 providing as output the drop volume V, the interfacial tension γ, and the interfacial area A.
194 The aqueous droplet was formed at the tip of the capillary and immersed in a glass cuvette,
195 which contained the oil phase, placed in a thermostatically controlled cell at 20 ºC. The
196 interfacial tension of the clean interface (oil–water) was measured before every experiment to
197 ensure the absence of surface-active contaminants obtaining values of (29.5 ± 0.5) mN/m at
198 20 ºC. The materials in contact with the solutions were properly cleaned in order to avoid any
199 contamination by any surface active substance.
200 Measurements of the interfacial dilatational rheology were made at the end of the adsorption
201 period by inducing sinusoidal oscillations to the interface, by injecting and extracting volume
202 into and from the droplet, while the response in the interfacial tension was recorded. The
203 dilatational parameters of the interfacial layers were calculated via a Fourier transformation
204 algorithm implemented in the software analysis. In a general case, the dilatational modulus
205 (E) is a complex quantity that contains a real and an imaginary part:

206 $$E = E' + iE'' = \varepsilon + i2\pi f\eta \quad (1)$$

207 where E' is the storage modulus or the elasticity (ε) of the interfacial layer and E'' is the loss
208 modulus that accounts for the viscosity (η) of the interfacial layer. The applied interfacial
209 area oscillations were maintained at 5 % of amplitude to avoid excessive perturbation of the
210 interfacial layer and the departure from the linear viscoelastic region (Camino, Perez,
211 Sanchez, Patino, & Pilosof, 2009; Mezdour, Lepine, Erazo-Majewicz, Ducept, & Michon,
212 2008). The oscillation frequency (f) ranged from 0.01 to 0.3 Hz.

The reproducibility of the experiments was verified from the standard deviation of at least three replicate measurements.

3. RESULTS AND DISCUSSION

Interactions between cellulose ethers and the bile salt will be studied separately in the aqueous phase and at the oil–water interface to account for different scenarios of an oil-in-water emulsion in the duodenum stage of digestion; that is the bulk phase and surface of oil droplets in the presence of bile salts. In addition, in both areas of study, corresponding to aqueous phase or oil–water interface, the behaviour of cellulose ethers alone will be considered, as a reference, before comparing with the behaviour of mixtures of cellulose ethers and bile salt.

3.1. Bulk properties of cellulose ethers

Firstly, the effect of the molecular weight on the bulk properties of cellulose alone is considered by comparing the micro-DSC traces for two samples with the same type and number of substituents but different range of viscosity and hence molecular weight. Namely, MC A4C (lower molecular weight) and A4M (higher molecular weight) are compared in Figure 1a. The thermograms of both types of MC display an endothermic peak on heating which appears exothermic on cooling. This thermal transition corresponds to the gelation process of MC, which has been previously characterised by a combination of techniques, such as DSC and rheology, by Haque and co-workers (Haque & Morris, 1993). As observed in Figure 1a, the temperature-course of thermogelation is comparable for both A4C and A4M upon heating and cooling. Furthermore, the transition enthalpy values measured from the area below the peaks on heating and on cooling for A4C and A4M, which are also shown in Figure 1, are similar within the margin of error. These observations can be explained by the

presumably similar content of hydrophobic substituents, *i.e.* methyl groups, in both types of MC and are therefore not molecular weight dependant.

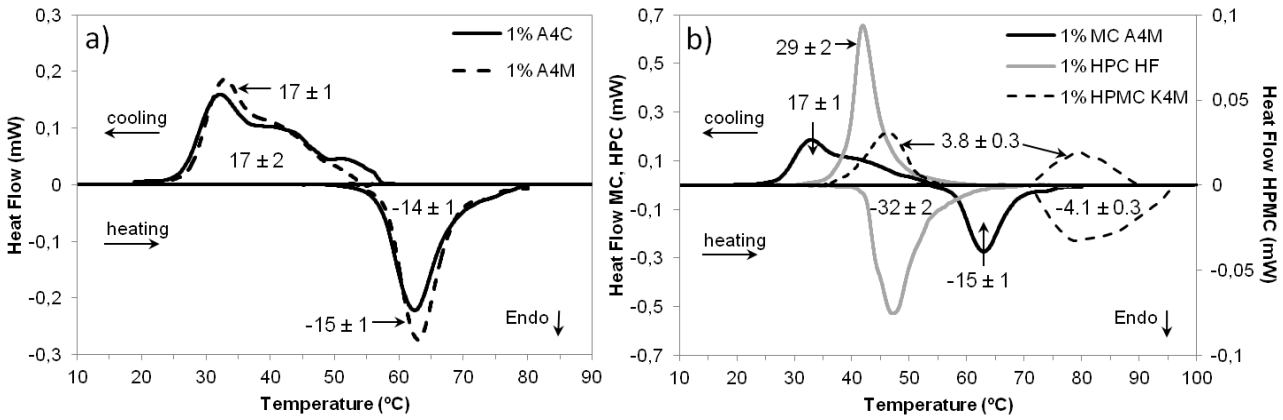

Figure 1: Micro-DSC traces on heating and on cooling of a) 1 wt% MC solutions: low molecular weight, A4C; high molecular weight, A4M; b) 1 wt% cellulose ether solutions; left axis: MC A4M; HPC HF; right axis: HPMC K4M. Transition enthalpy values on heating and on cooling are given in $J/g_{polymer}$.

Secondly, the effect of number and type of substituents on the bulk properties is evaluated for the set of cellulose ethers within a similar range of viscosity: MC A4M, HPMC K4M and HPC HF. Corresponding micro-DSC traces and the values of the transition enthalpy are presented in Figure 1b for A4M, K4M and HF at 1 wt%. MC and HPC will be first compared since they present different substituents, methyl or hydroxypropyl groups, respectively. Then, the effect of the presence of both kinds of substituents in HPMC will be discussed, comparing with the behaviour of MC and HPC. It can be seen in Figure 1b appreciable differences between the thermograms of HPC and MC. HPC shows the highest values of transition enthalpy, "demixes" at lower temperature on heating and displays slight thermal hysteresis when re-dissolving on cooling, as compared to MC. Previous studies proposed different mechanisms of thermal transition for cellulose ethers (Haque & Morris, 1993; Haque,

Richardson, Morris, Gidley, & Caswell, 1993; Sun et al., 2009), which are summarised here to explain the differences found for HPC and MC (Figure 2). In the case of HPC which is highly substituted (Table 1), the more "uniform" distribution of hydroxypropyl groups along the polymer chains would allow the hydrophobic association to take place in one step upon heating. Differently, gelation of MC comprises at least two steps. MC is found in solution as bundles where strands are held together by packing of unsubstituted regions and by hydrophobic clustering of methyl groups in regions of denser substitution. In a first step upon heating, the strands separate at the ends of the bundles and methyl groups are exposed. This allows the second step to take place upon further increasing temperature, that is, the association of hydrophobic regions of strands from different bundles (Figure 2).

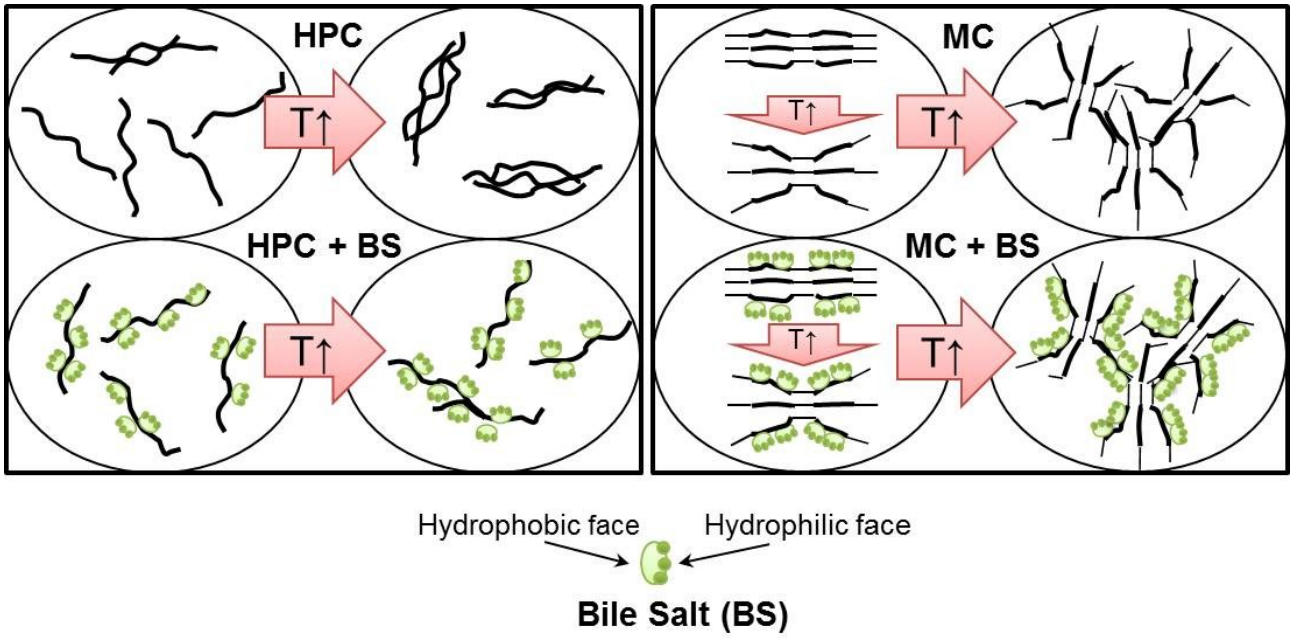

Figure 2: Schematic representation of the hypothetical structures and processes involved in the thermal transition of cellulose ethers, HPC and MC, in the absence and presence of the bile salt. Faint lines in cellulose ethers denote unsubstituted or sparingly substituted chain segments; bold lines denote regions of dense substitution. See text for detailed description.

On the other hand, HPMC shows the lowest values of the transition enthalpy and also gels at higher temperature on heating, as compared to MC (Figure 1b). The mechanism of thermogelation is similar to that for MC, however, differences can be explained not only by the lower content of hydrophobic substituents due to its lower DS for methyl groups, but also by the presence of more polar hydroxypropyl groups that inhibit the hydrophobic gelation (Haque et al., 1993). What Haque and co-workers did not show, that we now present in Figure 1b, is a high temperature exotherm for HPMC upon cooling. We tentatively ascribe this to possible distributions of the methyl and hydroxypropyl substituents on the cellulose bundles, which we are currently investigating. Hence, clearly the type, number and distribution of substituents affect the bulk properties of cellulose ethers (Sullo, Wang, Koschella, Heinze, & Foster, 2013) that may also affect the interactions with the bile salt, as it will be discussed below.

Finally, the effect of bulk concentration on the thermal transition of cellulose ethers is studied for MC (A4M) and HPC (HF) at 0.3 and 1 wt% (Figure 3). Micro-DSC traces of HPMC K4M at the relatively low concentration of 0.3 wt% were not reported here due to the low values of the transition enthalpy. It can be observed in Figure 3 that the temperature-course of the thermal event is independent of concentration for both types of cellulose ether, although transition-onset temperatures are slightly displaced to higher values when decreasing the bulk concentration, and transition enthalpy remains constant when normalised per gram of polymer. This behaviour will be useful when interpreting the data for cellulose ethers in the presence of bile salt.

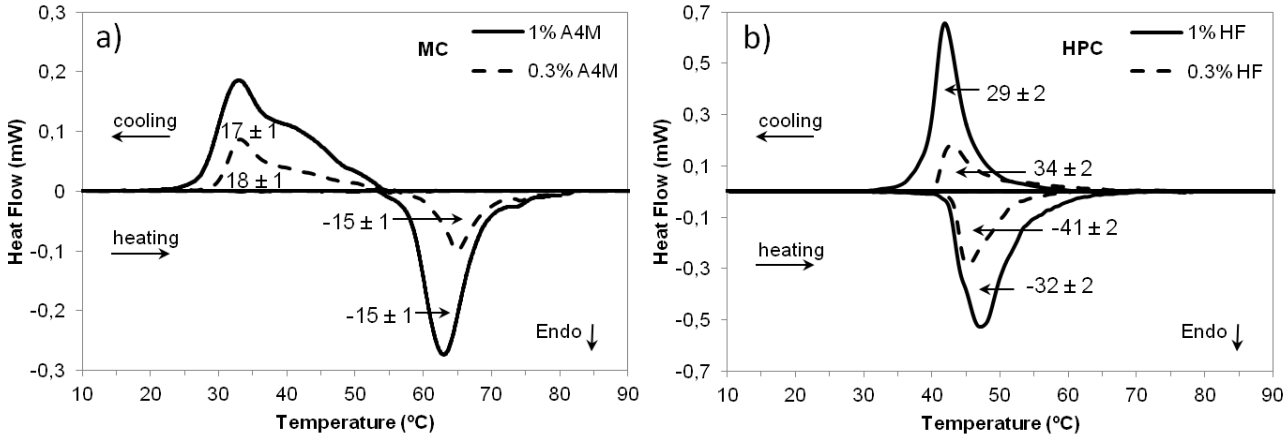

297

298 **Figure 3:** Micro-DSC traces on heating and on cooling of 0.3 and 1 wt% cellulose ether
299 solutions: a) MC A4M; b) HPC HF. Transition enthalpy values on heating and on cooling are
300 given in J/$g_{polymer}$.

301

302 *3.2. Interactions between cellulose ethers and bile salt in the aqueous phase*

303 In this section, similar micro-DSC experiments were carried out for mixtures of cellulose
304 ethers at a fixed concentration of 0.3 and 1 wt% and the bile salt at concentrations varying
305 from 0-100 mM in each case.

306 Figure 4 displays the peaks on heating and on cooling of cellulose ethers due to thermal
307 transitions, in the absence and in the presence of the bile salt. Cellulose ethers within the
308 same range of viscosity but with different number and type of substituents (MC A4M, HPMC
309 K4M and HPC HF) were chosen for these experiments, since the thermal transition appears
310 to be independent of the molecular weight for MC A4C and A4M. The most remarkable
311 result is that the peak size gradually decreases upon increasing the bile salt concentration and
312 even shift to higher temperatures, as observed in Figure 4. The shift is greater in the case of
313 HPC, as compared to MC. This trend is also observed when the concentration of cellulose
314 ethers was fixed at 0.3 wt% (data not shown). In the case of HPMC, the intermediate and
315 highest concentrations of NaTDC shift the peaks to even a larger extent than for HPC. It

316 seems that the bile salt interacts with cellulose ethers affecting or even inhibiting the thermal
317 transition, as seen for HPMC at a bile salt concentration of 100 mM (Figure 4b).
318

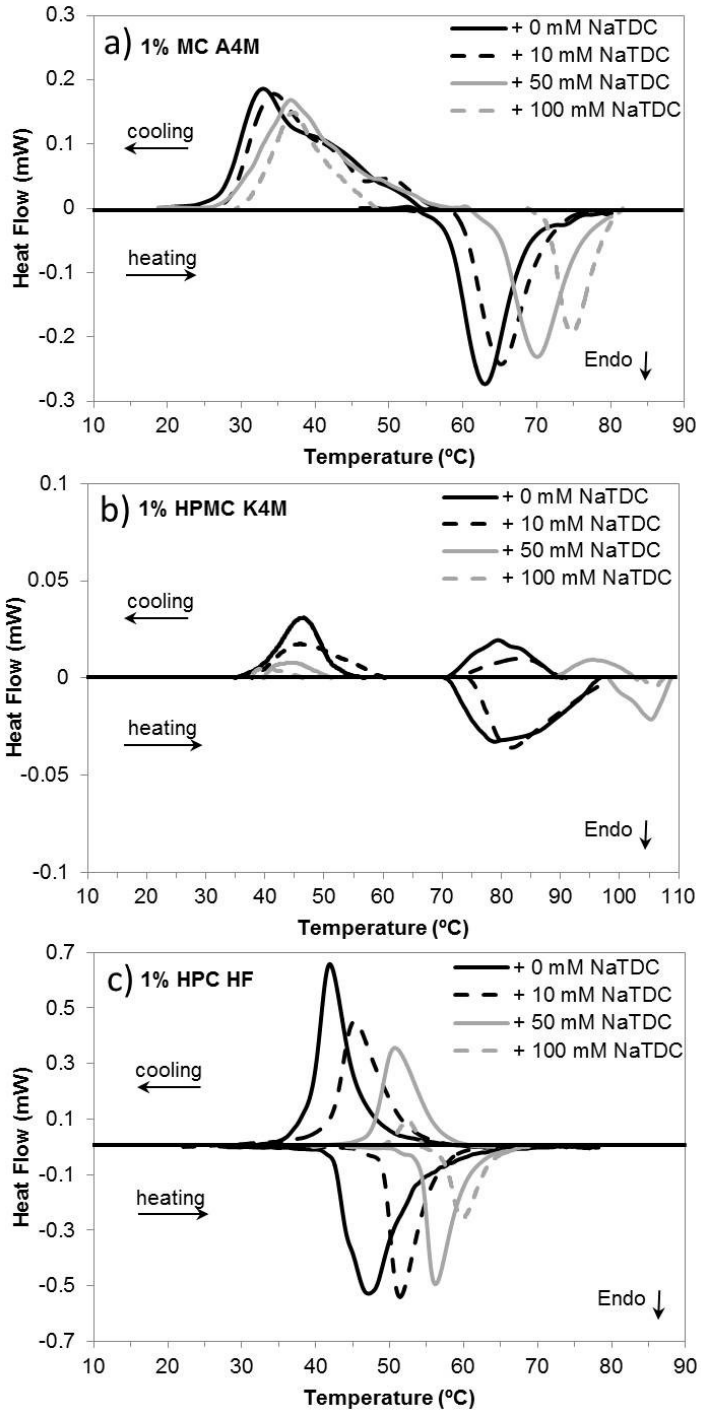

319
320 **Figure 4:** Micro-DSC traces on heating and on cooling of mixtures of 1 wt% cellulose ether
321 solutions and bile salt at several concentrations: a) MC A4M; b) HPMC K4M; c) HPC HF.
322

In order to analyse the effect of the type and number of substituents on these interactions with the bile salt, the decrease in the transition enthalpy of cellulose ethers on heating is plotted as a function of the bile salt concentration in Figure 5a. As a general trend, increasing the concentration of bile salt decreases the transition enthalpy of cellulose ethers. However, there are clear differences regarding the type and number of substituents. On the one hand, bile salt reduces the transition enthalpy to a larger extent for HPMC and HPC within the whole range of bile salt concentration, as compared to MC. As in the previous section, the effect of the bile salt on thermal transition of cellulose ethers will be first compared for MC and HPC, and then for HPMC.

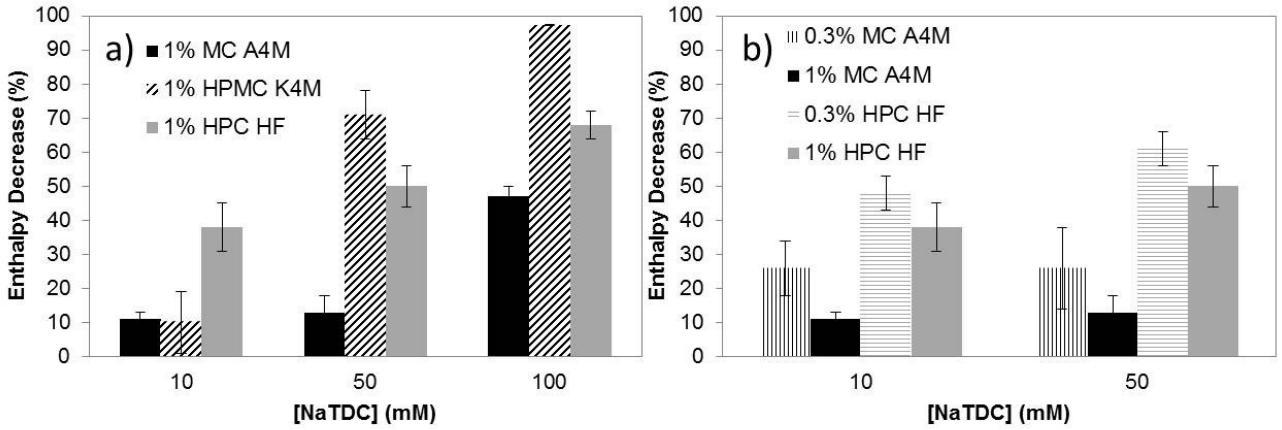

Figure 5: Decrease in transition enthalpy of cellulose ethers caused by the presence of the bile salt: a) effect of the type and number of substituents; b) effect of bulk concentration.

We propose the following mechanism of interaction between cellulose derivatives and the bile salt, which is illustrated in Figure 2, to explain the results, taking into account the model proposed by Haque and co-workers (Haque & Morris, 1993; Haque et al., 1993). The hydrophobic face of bile salt molecules adsorbs on the hydrophobic portions of cellulose ethers, while the hydrophilic face exposures to the aqueous phase. In the case of HPC, the more "uniform" distribution of bile salt along the polymer chains through the hydroxypropyl

groups would hinder the hydrophobic association upon heating. Differently for MC, bile salt would adsorb to the methyl groups in the regions of denser substitution. Upon heating, the recently exposed methyl groups would be still available, when the strands separate at the end of the bundles, for the hydrophobic association of strands from different bundles to take place (Figure 2). This then explains why the bile salt inhibits the thermal transition to a larger extent for HPC as compared to MC regardless of the bile salt concentration, as well as the larger shift of the peaks to higher temperature (Figures 4a,c; 5a). Next, the effect of the bulk concentration of cellulose ethers on these interactions with the bile salt will be evaluated. For this purpose, the decrease in the transition enthalpy of MC A4M and HPC HF is plotted for the two concentrations studied, 0.3 and 1 wt%, as a function of the bile salt concentration in Figure 5b. At a bulk concentration of 0.3 wt% for MC and HPC, again the bile salt decreases to a greater extent the transition enthalpy for HPC, at all bile salt concentrations, as compared to MC. This supports our hypothesis of interaction illustrated in Figure 2. However, the enthalpy reduction by the bile salt is larger for MC and HPC at 0.3 wt% than at 1 wt% (Figure 5b). This can be explained by the increase of the ratio bile salt/cellulose ether at this lower bulk concentration of cellulose derivatives. The cellulose ether concentrations tested in this study are well tolerated regarding future perspective of human health. On the other hand, the bile salt concentrations used: 10, 50 and 100 mM, are above the physiological concentration range in the fasted state in the human small intestine (3-7 mM). However, it involves the physiological concentration range in the fed state (up to 20 mM). Since the interactions between cellulose ethers and bile salt depend on the bile salt/cellulose ether ratio, the cellulose ether concentration must be decreased to test higher bile salt/cellulose ether ratios at physiological bile salt concentrations.

Finally, the mechanism of bile salt adsorption onto HPMC bundles would be similar to that on MC (Figure 2). However, the lower content of methyl groups in HPMC and the presence

368 of the more polar hydroxypropyl groups would explain the results observed in Figure 5a.
369 Namely, the reduction in the transition enthalpy of HPMC by bile salt is much larger at
370 higher NaTDC concentrations, as compared to MC. The gel formed by HPMC is
371 substantially weaker than MC gel due to the presence of the larger hydroxypropyl
372 substituents that inhibit intermolecular association (Haque et al., 1993). To recall,
373 thermogelation of HPMC does not occur until higher temperature and the transition enthalpy
374 is considerably lower than for MC (Figure 1b). Interestingly, the resistance of hydroxypropyl
375 groups to incorporation in ordered structures upon heating seems to be magnified in the
376 presence of the bile salt, as observed at the highest bile salt concentration where the gelation
377 of HPMC is completely inhibited (Figures 4b; 5a).
378
379 *3.3. Interfacial activity of cellulose ethers at the oil–water interface*
380 Before considering the competitive adsorption of cellulose derivatives and bile salt at the oil–
381 water interface, first the interfacial activity of cellulose ethers alone is evaluated as a
382 reference. Few investigations have been focused on the behaviour of these cellulose ethers at
383 the oil–water interface (Camino et al., 2009; Mezdour et al., 2008), and to our best
384 knowledge none of them focused on the combined study of the three types investigated here
385 or in their competitive adsorption with bile salts. For that reason, the values of interfacial
386 tension and dilatational modulus measured after 30 min of adsorption at 20 ºC are presented
387 as a function of the bulk concentration. These are not equilibrium values, since several hours
388 are needed to attain true equilibrium: from at least 12 to 24 h for low derivatised cellulose
389 concentrations (Camino et al., 2009; Persson, Nilsson, & Sundelof, 1996). A combination of
390 slow diffusion transport of polymer to the interface and slow conformational rearrangements
391 of already adsorbed polymer is thought to cause the slow decrease in the surface tension at
392 low concentrations (Nahringbauer, 1995). Nevertheless, the adsorption process is completed

393 within a very short timeframe, of the order of a few seconds, at high concentrations (Mezdour
394 et al., 2007). Since this work is part of an integral study where stabilisation of oil in water
395 emulsions is involved, interfacial parameters at short timescale, 30 min or less, will provide
396 relevant information to emulsification procedures.
397 As done for the experiments in the aqueous phase, the effect of the molecular weight is first
398 considered on the interfacial activity of cellulose ethers. The interfacial behaviour of MC
399 A4C and MC A4M is compared in Figure 6a. Both types of MC lower the interfacial tension
400 to a similar extent after 30 min of adsorption, reaching a saturation value of approximately 16
401 mN/m, which is in agreement with values reported for METHOCEL™ A4M at oil–water
402 interfaces (Floury, Desrumaux, Axelos, & Legrand, 2003; Gaonkar, 1991). This is
403 presumably due to the similar hydrophobicity of A4C and A4M since the content of methyl
404 groups is the same in both kinds of MC (Table 1). Previous work showed similar interfacial
405 tension for METHOCEL™ HPMC samples of different viscosities, suggesting an interfacial
406 activity independent of the molecular weight (Gaonkar, 1991). However, the adsorption
407 dynamics should depend on the molecular weight, since the diffusion to the interface is
408 slower for larger molecules (Floury et al., 2003). Indeed, initial adsorption rates at low MC
409 concentrations (10^{-5}-10^{-3} wt%) seem to be slightly slower for the higher molecular weight
410 A4M than for the lower molecular weight A4C (results not shown). Then, the complex
411 dilatational modulus is reported at a representative frequency of 0.1 Hz (Figure 6a), since a
412 predominantly elastic response, *i.e.* $E' > E''$, was obtained at all frequencies and
413 concentrations tested, as reported for some cellulose derivatives at the air–water interface
414 (Perez, Sanchez, Patino, & Pilosof, 2006). Furthermore, the loss tangent that represents the
415 relationship between the viscous and elastic component of the interfacial dilatational modulus
416 ($\mathrm{Tan}\delta = E''/E'$) appears frequency independent at high concentrations, $\mathrm{Tan}\delta \sim 0.2$, and
417 ranging from 0.2 to 0.4 at low concentrations (data not shown). A molecular weight-

418 dependence would be also expected for the viscoelasticity of MC interfacial layers (Floury et
419 al., 2003). At a certain interfacial concentration, the resistance to dilatation/compression
420 deformation depends on the interactions of the molecules adsorbed at the interface and
421 adsorption rate of molecules present in the surrounding aqueous phase, which in turn will
422 depend on the molecular size, among other properties. Interestingly, both types of MC
423 display the same dilatational response (Figure 6a). Similar viscoelasticity between HPMC
424 samples of different molecular weight but similar degree of methyl substitution was also
425 found by Pérez and co-workers (Perez et al., 2006). Hence, it seems that, in the studied
426 molecular weight range, the interactions between hydrophobic segments actually in contact
427 with the interface account for the measured dilatational modulus. It is then reasonable to
428 think that the similar dilatational response found for MCs might be due to similar proportion
429 of interacting methyl substituents adsorbed at the interface. The presence of two maxima in
430 the dilatational modulus (Figure 6a) suggests at least two changes in interfacial conformation
431 upon increasing the concentration. The first maximum is located at a bulk concentration
432 corresponding to the initial decrease in interfacial tension, just before the abrupt drop. The
433 formation of trains, loops and tails is likely to occur (Wollenweber, Makievski, Miller, &
434 Daniels, 2000), having rearrangements on the interfacial layer with adsorbed molecules going
435 from a more expanded configuration to a more condensed one (Li, Xu, Xin, Cao, & Wu,
436 2008; Perez et al., 2006). Then, the second maximum is found at a higher bulk concentration
437 corresponding to the plateau in the interfacial tension, where a saturated interface has been
438 reached. It seems that at higher interfacial coverage, MC molecules continue rearranging,
439 forming a more condensed interfacial layer or even multilayers, as reported for HPMC at air–
440 water and oil–water interfaces (Perez et al., 2006; Wollenweber et al., 2000).

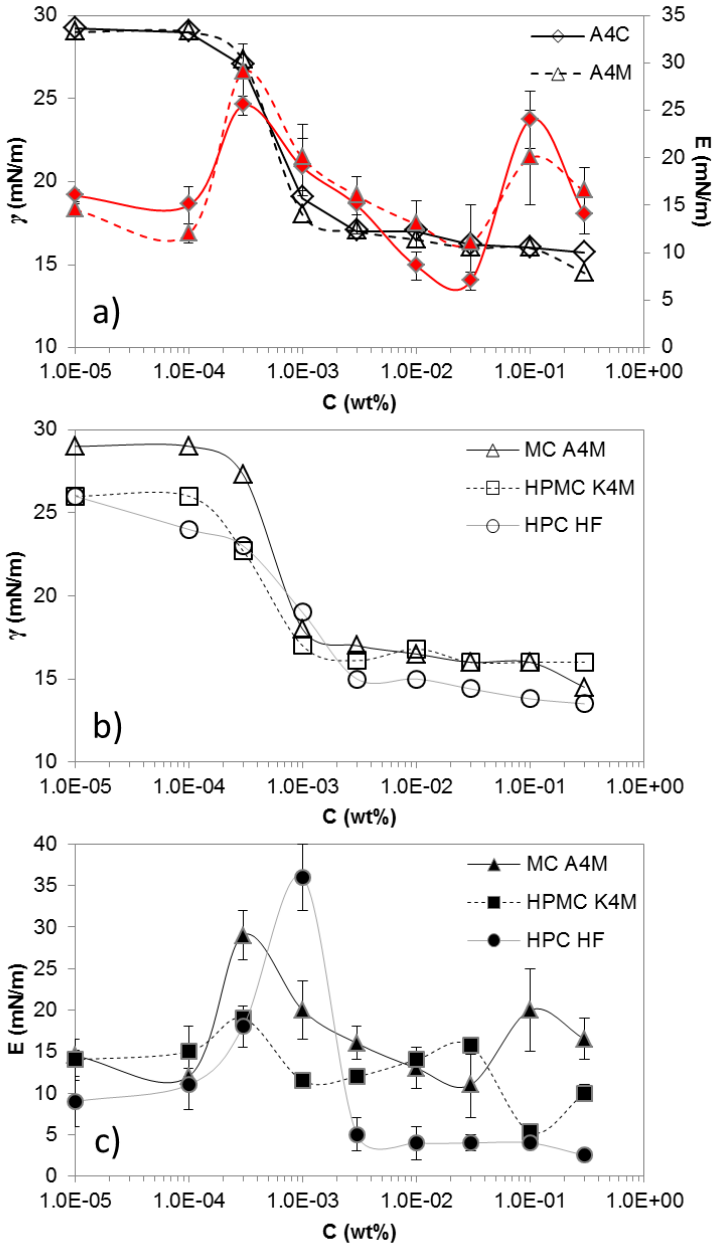

441

442 **Figure 6:** Interfacial tension (open symbols) and dilatational modulus (closed symbols) (f =
443 0.1 Hz) of a) MC solutions (low molecular weight, A4C; high molecular weight, A4M), b)
444 and c) cellulose ethers solutions (MC A4M; HPMC K4M; HPC HF) at the olive oil–water
445 interface as a function of the bulk concentration (T = 20 ºC, 30 min of adsorption). Error bars
446 are within the size of the symbols for the interfacial tension values.

447

448 Next, the effect of the type and number of substituents on the interfacial activity is evaluated
449 for the set of cellulose derivatives within the similar range of viscosity (Figure 6b,c). In this
450 case, appreciable differences can be observed in the interfacial behaviour. Interfacial activity
451 of MC and HPC are first compared. HPC lowers the interfacial tension to a larger extent than
452 MC within practically the whole range of concentration, after 30 min of adsorption (Figure
453 6b). Also, the initial decrease in the interfacial tension at lower concentrations is more
454 gradual for HPC. The larger number and size of hydroxypropyl groups in HPC would
455 eventually occupy larger interfacial area than methyl groups in MC, which is related with
456 larger decrease in the interfacial tension. Previous studies showed lower surface tension for
457 HPC, while MC and HPMC displayed similar but higher surface tension (Arboleya & Wilde,
458 2005; Mezdour et al., 2007; Persson et al., 1996). Hence, an analogous behaviour is found at
459 both air–water and oil–water interfaces. However, hydroxypropyl groups present a more
460 polar character than methyl groups, which is reflected in slower adsorption rates of HPC at
461 low bulk concentrations: 10^{-5}-10^{-2} wt% (data not shown). On the other hand, the breakpoint
462 of the interfacial tension between the low and high polymer concentration regimes, denoted
463 as critical aggregation concentration (CAC), which is characteristic for a given polymer, and
464 is related with the critical micelle concentration of low molecular weight surfactants, seems
465 to be higher for HPC. However, it has to be taken into account that these are not equilibrium
466 values. When the adsorption of a 10^{-3} wt% HPC solution was measured after 1 h, the
467 interfacial tension reached a value of 16.5 mN/m. Hence, this concentration is the CAC after
468 1 h of adsorption, for both MC and HPC. This agrees with the similar CAC values found for
469 HPC and different HPMCs, suggesting that the molecular weight and the type and degree of
470 substitution have a low influence on CAC (Persson et al., 1996; Wollenweber et al., 2000).
471 Regarding the dilatational behaviour (Figure 6c), some differences can be seen in the location
472 of the first maximum in the dilatational modulus at lower interfacial coverage and the missing

second maximum of HPC at higher interfacial coverage. The first maximum appears at higher bulk concentration for HPC than for MC, corresponding also to a larger decrease in the interfacial tension of HPC, as compared to the interfacial tension of MC. It is likely that HPC chains lay in a more expanded structure than MC at the interface, at lower concentrations, due to the more "uniform" distribution of substituents. This would also contribute to the larger decrease in the interfacial tension at lower interfacial coverage for HPC. Then, the polymer chains would rearrange, as in the case of MC, into a brush-like conformation upon increasing the interfacial coverage (Mezdour et al., 2008). However, HPC does not show the second maximum in the dilatational modulus as MC, suggesting that it does not change the interfacial configuration within the regime of high concentration. HPC interfacial structure might become more condensed instead, upon further increasing the bulk concentration, as seen by the continuous decrease in interfacial tension at higher interfacial coverage. Differently for MC, the formation of multilayers might be possible, as reflected by the second maximum (Figure 6c).

Finally, HPMC shows an interfacial behaviour which is in between of those of MC and HPC. Within the regime of low bulk concentration, the adsorption isotherm of HPMC is similar in shape to that of MC, although approaching interfacial tension values attained by HPC (Figure 6b). Adsorption dynamics of HPMC is slightly slower than for MC but faster than for HPC, corroborating that at a certain viscosity, the more hydrophobic methyl groups in the whole molecule act as a driving force for the diffusion (Perez, Sanchez, Pilosof, & Patino, 2008). In addition, the first maximum in the dilatational modulus is located at the same concentration as for MC, although shows lower values (Figure 6c). It seems that HPMC changes the interfacial conformation in a similar way as MC, suggested by the shape in the adsorption isotherm and the location of the dilatational modulus maximum, however the presence of hydroxypropyl groups occupying larger interfacial area than methyl groups might explain the

larger decrease in the interfacial tension as compared to MC. The saturation of the interfacial layer starts at the same bulk concentration of 10^{-3} wt% for MC and HPMC, in agreement with literature values at air–water interface (Arboleya & Wilde, 2005), and reaching similar values of the interfacial tension within the regime of high interfacial coverage (Figure 6b). Nevertheless, the second maximum in the dilatational modulus appears now at lower concentration for HPMC than for MC (Figure 6c). This suggests again a similar conformation to that acquired for MC upon increasing the concentration, such as multilayer formation, however now being attained at slightly lower interfacial coverage for HPMC. Hence, despite HPMC also forms similar bundles as MC in solution, the lower degree of substitution for methyl groups and the presence of hydroxypropyl groups clearly give rise to differences in the interfacial behaviour.

There is some evidence from these results that the interfacial properties of macromolecules like cellulose ethers at the oil–water interface depend on the length and distribution of trains, loops and tails, analogous to the behaviour at the air–water interface (Perez et al., 2006).

3.4. Competitive adsorption of cellulose ethers and bile salt at the oil–water interface

Finally, for the competitive adsorption experiments of cellulose ethers in the presence of the bile salt, we have chosen a fixed bulk concentration of cellulose derivatives of 10^{-3} wt%. Such a concentration provides an almost saturated interface, given by the value of the interfacial tension close to the plateau in the adsorption isotherm (Figure 6b), and a dilatational modulus close to the first maximum (Figure 6c), when a brush-like conformation has been reached. In this section, the interfacial tension and dilatational modulus of mixtures of cellulose ethers and bile salt after 30 min of adsorption at the oil–water interface are displayed as a function of the bile salt concentration (Figure 7). Results are discussed comparing with the interfacial behaviour of the bile salt alone, referred as control in Figure 7.

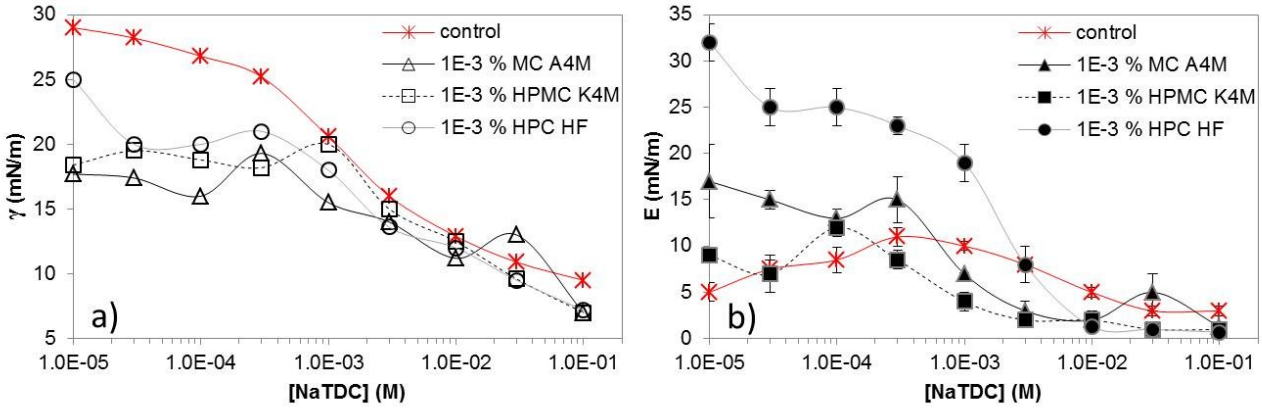

Figure 7: a) Interfacial tension (error bars are within the size of the symbols) and b) dilatational modulus (f = 0.1 Hz) of mixtures of 10^{-3} wt% cellulose ethers (MC A4M; HPMC K4M; HPC HF) and bile salt (NaTDC) solutions at the olive oil–water interface as a function of the bile salt bulk concentration (T = 20 ºC, 30 min of adsorption).

At the lowest bile salt concentration, mixtures attain interfacial tension (Figure 7a) and dilatational modulus (Figure 7b) values similar to those of cellulose ethers in the absence of the bile salt (Figure 6b,c). Also, the adsorption rate is similar to that for cellulose derivatives alone (data not shown). This means that the process of adsorption is being controlled by the cellulose derivatives and that the adsorbed layer is mainly composed of cellulose ethers even after 30 min of adsorption. The only exception is found for the mixture of HPC and bile salt, with higher interfacial tension than for HPC alone, although the dynamics of adsorption and dilatational modulus agree with that for HPC alone. When increasing the bile salt concentration in the mixtures, the rates of adsorption remain similar to those for cellulose ethers alone, however the dynamic and final interfacial tension start to be affected when approaching the concentration of bile salt of 10^{-3} M. It can be seen that upon further increasing the concentration of bile salt in the mixtures, adsorption isotherms (Figure 7a) and dilatational moduli (Figure 7b) of mixed systems approach those of pure bile salt, *i.e.* control.

In addition, the adsorption dynamics are similar to those of bile salt alone at the different concentrations, *i.e.* fast initial adsorption rates attaining a steady interfacial tension in less than 2 min, as compared with cellulose ethers which attain a steady interfacial tension in at least 10 min at the concentration of 10^{-3} wt% (results not shown). This suggests that the adsorption is being controlled by the bile salt. This physiological surfactant is very efficient at occupying the oil–water interface, competing with other surface active molecules or even displacing those already adsorbed at the interface, due to a combination of fast adsorption and planar shape (Maldonado-Valderrama et al., 2011; Torcello-Gómez, Jódar-Reyes, Maldonado-Valderrama, & Martin-Rodriguez, 2012). The order in which the molecules arrive at the interface will influence the final interfacial composition (Damodaran & Rammovsky, 2003; Ridout, Mackie, & Wilde, 2004). However, the composition of the interface may change with time. Molecules that are initially at the interface may be displaced by the molecules in the bulk that have a greater affinity for the interface (Baeza, Sanchez, Pilosof, & Patino, 2005). Here, it seems that although bile salts are controlling the rates of adsorption from the initial moments, cellulose ethers are also contributing to the decrease of the interfacial tension since a lower value is obtained, as compared to the behaviour of bile salt alone, throughout the whole process of adsorption (results not shown). Interestingly, even at the highest bile salt concentration, the mixtures lower the interfacial tension to a larger extent than pure bile salt, and also show lower dilatational response, meaning a less elastic and less structured interface. This indicates coexistence of both cellulose and bile salt at the oil–water interface. It might be possible that the presence of interfacial derivatised cellulose–bile salt complexes account for this further decrease in the interfacial tension, with a synergistic effect. Similar properties were found in our previous study on competitive adsorption between triblock copolymers and this bile salt at the olive oil–water interface (Torcello-Gómez et al., 2013). We have proven that all types of cellulose ethers studied in the

current work are able to compete for a hydrophobic interface with the bile salt. This is a very important result from the viewpoint of controlling lipid digestibility, since cellulose derivatives may compete with the bile salts for the oil–water interface of emulsified lipids within the duodenum. The ability of derivatised cellulose to adsorb to an oil–water interface in the presence of bile salts might be partially due to the sequestration of bile salts in the bulk through the binding to cellulose ethers, as indicated by micro-DSC experiments of mixed systems in the aqueous phase.

CONCLUSIONS

We have proven that the presence of bile salt affects the thermal transition undergone by cellulose ethers upon heating and cooling. This inhibition by the bile salt depends on the mechanism of thermogelation, which in turn will be determined by the type and number of substituents in cellulose ethers. The effect is increased by increasing the ratio bile salt/cellulose ether. Thermogelation of MC seems to be less susceptible to the presence of bile salt than HPMC and HPC, due to the hidden methyl groups in the bundles, which allow the intermolecular association to take place after exposing them upon heating. This inhibition in thermal transition of cellulose derivatives reflects that interactions between bile salt and cellulose ethers are taking place in the aqueous phase, supporting the mechanism of binding of bile salt to dietary fibre. They might also have implications in the control of lipid digestion in the sense that may have an impact on the surface of lipid droplets in emulsions, since cellulose ethers compete with the bile salt for the oil–water interface even at high bile salt concentrations relevant to physiological conditions within the duodenum.

These findings would allow the development of both functional foods and pharmacological matrices with tailored biological activities, such as control of satiety and targeted release of bioactive components to specific locations in the gastrointestinal tract.

ACKNOWLEDGEMENTS

Authors thank the financial support from the European Community's Seventh Framework Program (FP7-PEOPLE-2012-IEF) under Grant Agreement No. 326581. They thank Dr. Bettina Wolf for providing stimulating discussions.

REFERENCES

Anderson, J. W., & Siesel, A. E. (1990). Hypocholesterolemic Effects of Oat Products. In I. Furda, & C. J. Brine (Eds.), *New Developments in Dietary Fiber: Physiological, and Analytical Aspects* (Vol. 270, pp. 17-36). New York: Plenum Press.

Arboleya, J. C., & Wilde, P. J. (2005). Competitive adsorption of proteins with methylcellulose and hydroxypropyl methylcellulose. *Food Hydrocolloids, 19*(3), 485-491.

Baeza, R., Sanchez, C. C., Pilosof, A. M. R., & Patino, J. M. R. (2005). Interactions of polysaccharides with beta-lactoglobulin adsorbed films at the air-water interface. *Food Hydrocolloids, 19*(2), 239-248.

Beysseriat, M., Decker, E. A., & McClements, D. J. (2006). Preliminary study of the influence of dietary fiber on the properties of oil-in-water emulsions passing through an in vitro human digestion model. *Food Hydrocolloids, 20*(6), 800-809.

Camino, N. A., Perez, O. E., Sanchez, C. C., Patino, J. M. R., & Pilosof, A. M. R. (2009). Hydroxypropylmethylcellulose surface activity at equilibrium and adsorption dynamics at the air-water and oil-water interfaces. *Food Hydrocolloids, 23*(8), 2359-2368.

Damodaran, S., & Rammovsky, L. (2003). Competitive adsorption and thermodynamic incompatibility of mixing of beta-casein and gum arabic at the air-water interface. *Food Hydrocolloids, 17*(3), 355-363.

617 Fave, G., Coste, T. C., & Armand, M. (2004). Physicochemical properties of lipids: New
618 strategies to manage fatty acid bioavailability. *Cellular and Molecular Biology, 50*(7), 815-
619 831.
620 Floury, J., Desrumaux, A., Axelos, M. A. V., & Legrand, J. (2003). Effect of high pressure
621 homogenisation on methylcellulose as food emulsifier. *Journal of Food Engineering, 58*(3),
622 227-238.
623 Gaonkar, A. G. (1991). Surface and Interfacial Activities and Emulsion Characteristics of
624 Some Food Hydrocolloids. *Food Hydrocolloids, 5*(4), 329-337.
625 Gunness, P., Flanagan, B. M., & Gidley, M. J. (2010). Molecular interactions between cereal
626 soluble dietary fibre polymers and a model bile salt deduced from C-13 NMR titration.
627 *Journal of Cereal Science, 52*(3), 444-449.
628 Haque, A., & Morris, E. R. (1993). Thermogelation of Methylcellulose .1. Molecular-
629 Structures and Processes. *Carbohydrate Polymers, 22*(3), 161-173.
630 Haque, A., Richardson, R. K., Morris, E. R., Gidley, M. J., & Caswell, D. C. (1993).
631 Thermogelation of Methylcellulose .2. Effect of Hydroxypropyl Substituents. *Carbohydrate*
632 *Polymers, 22*(3), 175-186.
633 Jenkins, D. J. A., Kendall, C. W. C., & Ransom, T. P. P. (1998). Dietary fiber, the evolution
634 of the human diet and coronary heart disease. *Nutrition Research, 18*(4), 633-652.
635 Kritchevsky, D., & Story, J. A. (1993). Influence of dietary fiber on cholesterol metabolism
636 in experimental animals. In G. A. Spiller (Ed.), *CRC Handbook of Dietary Fiber in Human*
637 *Nutrition* (pp. 163-178). Boca Raton: CRC Press.
638 Lairon, D. (1996). Dietary fibres: Effects on lipid metabolism and mechanisms of action.
639 *European Journal of Clinical Nutrition, 50*(3), 125-133.
640 Lee, J. K., Kim, S. U., & Kim, J. H. (1999). Modification of chitosan to improve its
641 hypocholesterolemic capacity. *Bioscience Biotechnology and Biochemistry, 63*(5), 833-839.

642 Li, Y. M., Xu, G. Y., Xin, X., Cao, X. R., & Wu, D. (2008). Dilational surface viscoelasticity
643 of hydroxypropyl methyl cellulose and C(n)TAB at air-water surface. *Carbohydrate*
644 *Polymers, 72*(2), 211-221.
645 Maldonado-Valderrama, J., Wilde, P., Macierzanka, A., & Mackie, A. (2011). The role of
646 bile salts in digestion. *Advances in Colloid and Interface Science, 165*(1), 36-46.
647 Mezdour, S., Cuvelier, G., Cash, M. J., & Michon, C. (2007). Surface rheological properties
648 of hydroxypropyl cellulose at air-water interface. *Food Hydrocolloids, 21*(5-6), 776-781.
649 Mezdour, S., Lepine, A., Erazo-Majewicz, P., Ducept, F., & Michon, C. (2008). Oil/water
650 surface rheological properties of hydroxypropyl cellulose (HPC) alone and mixed with
651 lecithin: Contribution to emulsion stability. *Colloids and Surfaces a-Physicochemical and*
652 *Engineering Aspects, 331*(1-2), 76-83.
653 Nahringbauer, I. (1995). Dynamic surface tension of aqueous polymer solutions .1.
654 Ethyl(hydroxyethyl)cellulose (BERMOCOLL cst-103). *Journal of Colloid and Interface*
655 *Science, 176*(2), 318-328.
656 Perez, O. E., Sanchez, C. C., Patino, J. M. R., & Pilosof, A. M. R. (2006). Thermodynamic
657 and dynamic characteristics of hydroxypropylmethylcellulose adsorbed films at the air-water
658 interface. *Biomacromolecules, 7*(1), 388-393.
659 Perez, O. E., Sanchez, C. C., Pilosof, A. M. R., & Patino, J. M. R. (2008). Dynamics of
660 adsorption of hydroxypropyl methylcellulose at the air-water interface. *Food Hydrocolloids,*
661 *22*(3), 387-402.
662 Persson, B., Nilsson, S., & Sundelof, L. O. (1996). On the characterization principles of some
663 technically important water-soluble nonionic cellulose derivatives .2. Surface tension and
664 interaction with a surfactant. *Carbohydrate Polymers, 29*(2), 119-127.
665 Reis, P., Holmberg, K., Watzke, H., Leser, M. E., & Miller, R. (2009). Lipases at interfaces:
666 A review. *Advances in Colloid and Interface Science, 147-48*, 237-250.

667 Ridout, M. J., Mackie, A. R., & Wilde, P. J. (2004). Rheology of mixed beta-casein/beta-
668 lactoglobulin films at the air-water interface. *Journal of Agricultural and Food Chemistry,*
669 *52*(12), 3930-3937.
670 Sarkar, N. (1979). Thermal Gelation Properties of Methyl and Hydroxypropyl
671 Methylcellulose. *Journal of Applied Polymer Science, 24*(4), 1073-1087.
672 Story, J. A., Furumoto, E. J., & Buhman, K. K. (1997). Dietary fiber and bile acid
673 metabolism - an update. In D. Kritchevsky, & C. Bonfield (Eds.), *Dietary Fiber in Health*
674 *and Disease* (Vol. 427, pp. 259-266). New York: Plenum Press.
675 Sullo, A., Wang, Y. H., Koschella, A., Heinze, T., & Foster, T. J. (2013). Self-association of
676 novel mixed 3-mono-O-alkyl cellulose: Effect of the hydrophobic moieties ratio.
677 *Carbohydrate Polymers, 93*(2), 574-581.
678 Sun, S. M., Foster, T. J., MacNaughtan, W., Mitchell, J. R., Fenn, D., Koschella, A., &
679 Heinze, T. (2009). Self-Association of Cellulose Ethers with Random and Regioselective
680 Distribution of Substitution. *Journal of Polymer Science Part B-Polymer Physics, 47*(18),
681 1743-1752.
682 Thongngam, M., & McClements, D. J. (2005). Isothermal titration calorimetry study of the
683 interactions between chitosan and a bile salt (sodium taurocholate). *Food Hydrocolloids,*
684 *19*(5), 813-819.
685 Tokle, T., Lesmes, U., Decker, E. A., & McClements, D. J. (2012). Impact of dietary fiber
686 coatings on behavior of protein-stabilized lipid droplets under simulated gastrointestinal
687 conditions. *Food & Function, 3*(1), 58-66.
688 Torcello-Gómez, A., Jódar-Reyes, A. B., Maldonado-Valderrama, J., & Martin-Rodriguez,
689 A. (2012). Effect of emulsifier type against the action of bile salts at oil-water interfaces.
690 *Food Research International, 48*(1), 140-147.

Torcello-Gómez, A., Maldonado-Valderrama, J., Jódar-Reyes, A. B., & Foster, T. J. (2013). Interactions between Pluronics (F127 and F68) and Bile Salts (NaTDC) in the Aqueous Phase and the Interface of Oil-in-Water Emulsions. *Langmuir, 29*(8), 2520-2529.

Vahouny, G. V., Satchithanandam, S., Chen, I., Tepper, S. A., Kritchevsky, D., Lightfoot, F. G., & Cassidy, M. M. (1988). Dietary Fiber and Intestinal Adaptation - Effects on Lipid Absorption and Lymphatic Transport in the Rat. *American Journal of Clinical Nutrition, 47*(2), 201-206.

Wollenweber, C., Makievski, A. V., Miller, R., & Daniels, R. (2000). Adsorption of hydroxypropyl methylcellulose at the liquid/liquid interface and the effect on emulsion stability. *Colloids and Surfaces a-Physicochemical and Engineering Aspects, 172*(1-3), 91-101.

Yokoyama, W., Anderson, W. H. K., Albers, D. R., Hong, Y. J., Langhorst, M. L., Hung, S. C., Lin, J. T., & Young, S. A. (2011). Dietary Hydroxypropyl Methylcellulose Increases Excretion of Saturated and Trans Fats by Hamsters Fed Fast Food Diets. *Journal of Agricultural and Food Chemistry, 59*(20), 11249-11254.

Zarras, P., & Vogl, O. (1999). Polycationic salts as bile acid sequestering agents. *Progress in Polymer Science, 24*(4), 485-516.

716 FIGURE CAPTIONS:

717 **Figure 1:** Micro-DSC traces on heating and on cooling of a) 1 wt% MC solutions: low
718 molecular weight, A4C; high molecular weight, A4M; b) 1 wt% cellulose ether solutions; left
719 axis: MC A4M; HPC HF; right axis: HPMC K4M. Transition enthalpy values on heating and
720 on cooling are given in $J/g_{polymer}$.

721

722 **Figure 2:** Schematic representation of the hypothetical structures and processes involved in
723 the thermal transition of cellulose ethers, HPC and MC, in the absence and presence of the
724 bile salt. Faint lines in cellulose ethers denote unsubstituted or sparingly substituted chain
725 segments; bold lines denote regions of dense substitution. See text for detailed description.

726

727 **Figure 3:** Micro-DSC traces on heating and on cooling of 0.3 and 1 wt% cellulose ether
728 solutions: a) MC A4M; b) HPC HF. Transition enthalpy values on heating and on cooling are
729 given in $J/g_{polymer}$.

730

731 **Figure 4:** Micro-DSC traces on heating and on cooling of mixtures of 1 wt% cellulose ether
732 solutions and bile salt at several concentrations: a) MC A4M; b) HPMC K4M; c) HPC HF.

733

734 **Figure 5:** Decrease in transition enthalpy of cellulose ethers caused by the presence of the
735 bile salt: a) effect of the type and number of substituents; b) effect of bulk concentration.

736

737 **Figure 6:** Interfacial tension (open symbols) and dilatational modulus (closed symbols) (f =
738 0.1 Hz) of a) MC solutions (low molecular weight, A4C; high molecular weight, A4M), b)
739 and c) cellulose ethers solutions (MC A4M; HPMC K4M; HPC HF) at the olive oil–water

740 interface as a function of the bulk concentration (T = 20 ºC, 30 min of adsorption). Error bars
741 are within the size of the symbols for the interfacial tension values.
742
743 **Figure 7:** a) Interfacial tension (error bars are within the size of the symbols) and b)
744 dilatational modulus (f = 0.1 Hz) of mixtures of 10^{-3} wt% cellulose ethers (MC A4M; HPMC
745 K4M; HPC HF) and bile salt (NaTDC) solutions at the olive oil–water interface as a function
746 of the bile salt bulk concentration (T = 20 ºC, 30 min of adsorption).
747